Experimental and Theoretical Studies on Ferromagnetically Coupled Metal Complexes with Imino Nitroxides

Hiroki Oshio,*,† Masashi Yamamoto,‡ Tasuku Ito,‡ Hidekazu Kawauchi,§ Nobuaki Koga,§ Tadaaki Ikoma,# and Shozo Tero-Kubota#

Department of Chemistry, University of Tsukuba, Tennodai 1−1−1, Tsukuba 305-8571, Japan, Department of Chemistry, Graduate School of Science, Tohoku University, Aoba-ku, Sendai 980-8578, Japan, Graduate School of Human Informatics, Nagoya University, Nagoya 464-8601, Japan, and Institute for Chemical Reaction Science, Tohoku University, Aoba-ku Sendai 980-8578, Japan

Received March 1, 2001

Copper(II), zinc(II), and nickel(II) complexes with tridentate imino nitroxyl diradicals, [CuCl(bisimpy)(MeOH)]-(PF_6) (**1**), [$ZnCl_2$(bisimpy)] (**2**), and [NiCl(bisimpy)(H_2O)$_2$]Cl·2H_2O (**3**) (bisimpy = 2,6-bis(1′-oxyl-4′,4′,5′,5′-tetramethyl-4′,5′-dihydro-1′*H*-imidazol-2′-yl)pyridine), were prepared, and their magnetic properties were studied. In **1**, the Cu(II) ion has a square pyramidal coordination geometry, of which the equatorial coordination sites are occupied by three nitrogen atoms from the bisimpy and a chloride ion. The coordination geometry of the Zn(II) ion in **2** can be described as a trigonal bipyramid, with two chloride ions and a bisimpy. In **3**, the Ni(II) ion has a distorted octahedral coordination geometry, of which four coordination sites are coordinated by the bisimpy and chloride ion, and two water molecules occupy the remaining cis positions. Magnetic susceptibility and EPR measurements revealed that in **1** and **3** the Cu(II) and Ni(II) ions with imino nitroxyl diraicals were ferromagnetically coupled, with the coupling constants J ($H = -2J_{ij}\sum S_iS_j$) of +165(1) and 109(2) cm^{-1}, respectively, and the intraligand ferromagnetic interactions in **1**−**3** were very weak. DFT molecular orbital calculations were performed on the diradical ligand, **1**, and **2** to study the spin density distribution before and after coordination to the metal ions.

Introduction

Interest in the magnetochemistry of metal complexes with organic radicals stems from the discovery of the molecule-based magnets, [Mn(hfac)$_2$(NIT−R)] (NIT−R = nitronyl nitroxide with an isopropyl group)[1] and [Fe(Me_5C_5)$_2$][TCNE]·MeCN.[2] Magnetic interactions between a metal ion and an organic radical depend on the magnetic orbital of the metal ion and coordination mode. Cu^{2+} or Ni^{2+} ions, having only dσ spins, often show ferromagnetic interactions with π radicals,[3] while a metal ion with dπ spins favors antiferromagnetic interactions with π radicals.[4] Therefore, molecule-based ferro- or ferrimagnets[5] and high-spin molecules[6] can be designed by choosing the proper combination of metal ion and organic radical.

In the analysis of a multiparamagnetic system, direct and indirect interactions between paramagnetic centers should be taken into account.[7] When the magnetic orbitals of each paramagnetic center have direct overlap, an antiferromagnetic interaction is always operative. When the paramagnetic centers are separated by bridges, the magnetic interaction depends on the nature of the bridges, and superexchange and spin-polarization mechanisms play an important role in determining the magnetic interaction. When the magnetic orbitals have an indirect overlap through the bridges, the paramagnetic centers

* To whom correspondence should be addressed.
† Department of Chemistry, University of Tsukuba.
‡ Department of Chemistry, Graduate School of Science, Tohoku University.
§ Graduate School of Human Informatics, Nagoya University.
# Institute for Chemical Reaction Science, Tohoku University.

(1) (a) Caneschi, A.; Gatteschi, D.; Rey, P.; Sessoli, R. *Inorg. Chem.* **1988**, *27*, 1756. (b) Caneschi, A.; Gatteschi, D.; Rey, P.; Sessoli, R. *Inorg. Chem.* **1988**, *27*, 3314. (c) Caneschi, A.; Gatteschi, D.; Rey, P.; Sessoli, R. *Acc. Chem. Res.* **1989**, *22*, 392. (d) Caneschi, A.; Gatteschi, D.; Renard, J.-P. Rey, P.; Sessoli, R. *J. Am. Chem. Soc.* **1989**, *111*, 785. (f) Vaz, M. G. F.; Pinheiro, L. M. M.; Stumph, H. O.; Alcântara, A. F. C.; Stéphane, G.; Ouahab, L.; Cador, O.; Mathonière, C.; Kahn, O. *Chem. Eur. J.* **1999**, *5* 1486. (g) Rancurel, C.; Leznoff, D. B.; Sutter, J.-P.; Gohlhen, S.; Ouahab, L.; Kliava, J.; Kahn, O. *Inorg. Chem.* **1999**, *38*, 4758. (h) Rancurel, C.; Leznoff, D. B.; Sutter, J.-P.; Guionneau, P.; Chasseau, D.; Kliava, J.; Kahn, O. *Inorg. Chem.* **2000**, *39*, 1602. (i) Inoue, K.; Iwamura, H. *J. Am. Chem. Soc.* **1994**, *116*, 3173. (j) Sakane, A.; Kumada, H.; Karasawa, S.; Koga, N.; Iwamura, H. *Inorg. Chem.* **2000**, *39*, 2891.

(2) Miller, J. S.; Calabrese, J. C.; Rommelmann, H.; Chittipeddi, S. R.; Zhang, J. H.; Reiff, W. M.; Epstein, A. J. *J. Am. Chem. Soc.* **1987**, *109*, 769.

(3) (a) Luneau, D.; Rey, P.; Laugier, J.; Fries, P.; Caneschi, A.; Gatteschi, D.; Sessoli, R. *J. Am. Chem. Soc.* **1991**, *113*, 1245. (b) Luneau, D.; Rey, P.; Belorizky, E.; Congne, A. *Inorg. Chem.* **1992**, *31*, 3578. (c) Luneau, D.; Romero, F. M.; Ziessel, R. *Inorg. Chem.* **1998**, *37*, 5078.

(4) (a) Fettouhi, M.; Khaled, M.; Waheed, A.; Golhen, S.; Ouahab, L.; Sutter, J.-P.; Kahn, O. *Inorg. Chem.* **1999**, *38*, 3967. (b) Lescop, C.; Luneau, D.; Belorizky, E.; Fries, P.; Guillot, M.; Rey, P. *Inorg. Chem.* **1999**, *38*, 5472.

(5) (a) Vaz, M. G. E.; Pinheiro, L. M. M.; Stumph, H. O.; Alcântara, A. F. C.; Golhen, S.; Ouahab, L.; Cador, O.; Mathonière, C.; Kahn, O. *Chem. Eur. J.* **1999**, *5*, 1486. (b) Fegy, K.; Luneau, D.; Belorizky, E.; Novac, M.; Tholence, J.-L.; Paulsen, X.; Ohm, T.; Rey, P. *Inorg. Chem.* **1998**, *37*, 4524. (c) Iwamura, H.; Inoue, K.; Koga, N. *New J. Chem.* **1998**, 201.

(6) (a) Vostrikova, K. E.; Luneau, D.; Wernsdorfer, W.; Rey, P.; Verdaguer, M. *J. Am. Chem. Soc.* **2000**, *122*, 718. (b) Marvilliers, A.; Pei, Y.; Boquera, J. C.; Vostrikova, K. E.; Paulsen, C.; Rivière, E.; Audierè, J.-P.; Mallah, T. *Chem. Commun.* **1999**, 1951. (b) Caneschi, A.; Gatteschi, D.; Laugier, J.; Rey, P.; Sessoli, R.; Zanchini, C. *J. Am. Chem. Soc.* **1988**, *110*, 2795.

(7) (a) Kahn, O. "Molecular Magnetism" VCH Publishers Inc.: New York, 1993. (b) Miller, J. S., and Epstein, A. J. *Angew. Chem., Int. Ed. Engl.* **1994**, *33*, 385.

10.1021/ic0102384 CCC: $20.00
Published on Web 09/18/2001

have an antiferromagnetic interaction. This indirect overlap is often accompanied with charge transfer between a paramagnetic center and a bridge, which is called a superexchange mechanism. In the absence of charge transfer, spin polarization becomes important and appears in multiradical organic compounds. Spin polarization occurs as a result of differing amplitudes of electrostatic repulsion between $\alpha\alpha$ and $\alpha\beta$ spins, where the former is smaller than the latter. The spin-polarization mechanism is a useful tool in predicting the sign of the magnetic interaction between radical centers.[8] For example, diradicals of *m*- and *p*- (or *o*-) xylene have ferromagnetic and antiferromagnetic interactions, respectively. Recently, spin polarization in multiradical systems was theoretically investigated using DFT (density functional theory), and the computational results were confirmed by polarized neutron diffraction (PND) experiments.[9] Although DFT and PND studies on a titanium(IV) (d^0) complex TiL_2 (L = tridentate dianion of semiquinone ligand) were reported,[10] DFT calculations on radical complexes with paramagnetic metal ions have been rarely done because it is a rather taxing calculation. Furthermore, little is known about the spin density distribution changes before and after coordination to metal ions, although the organic monoradicals,[11] diradicals,[12] and oligoradical ligands[13] have often been used as bridging moieties. In this article, we report the magnetic properties of metal complexes with a diradical ligand, [CuCl(bisimpy)(MeOH)](PF_6) (**1**), [$ZnCl_2$(bisimpy)] (**2**), and [NiCl(bisimpy)($H_2O)_2$]Cl·$2H_2O$ (**3**) (bisimpy = 2,6-bis(1′-oxyl-4′,4′,5′,5′-tetramethyl-4′,5′-dihydro-1′*H*-imidazol-2′-yl)pyridine).Theoretical studies using density function theory (DFT) calculations were performed to explore the nature of the spin polarization upon coordination of the ligand to the metal ions.

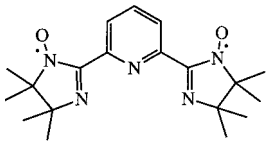

bisimpy

Results and Discussion

Structures of [CuCl(bisimpy)(MeOH)](PF_6) (1), [$ZnCl_2$-(bisimpy)] (2), and [NiCl(bisimpy)($H_2O)_2$]Cl·$2H_2O$ (3). Ortep diagrams of complexes **1** − **3** are, respectively, depicted in Figures 1 −3, and selected bond distances and angles are summarized in Tables 1 −3.

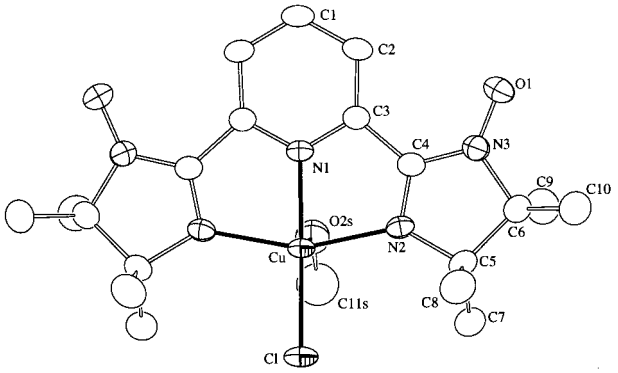

Figure 1. Ortep diagram (30% probability) of [CuCl(bisimpy)-(MeOH)]$^+$ in **1**.

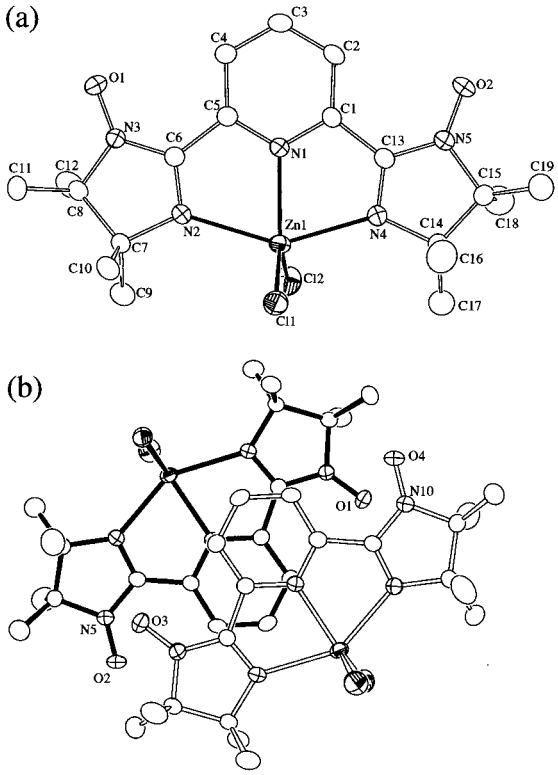

Figure 2. Ortep diagrams (30% probability) of (a)[$ZnCl_2$(bisimpy)] (**2**) and (b) the dimeric stack.

Complex **1** crystallized in the orthorhombic space group $Cmc2_1$ and is positioned on a mirror plane. The coordination geometry about the Cu(II) ion is a square pyramid, in which the equatorial sites are occupied by a chloride ion and three nitrogen atoms from bisimpy, and a methanol coordinates to the Cu(II) ion in the apical position.

The Cu−N2(imino nitroxide) bond is slightly longer (2.069-(2) Å) than the Cu−N1(pyridine) bond (1.979(2) Å), and the Cu−Cl bond length is 2.2226(7). The coordination bond lengths with equatorial atoms are shorter than those with apical oxygen atoms (Cu−O2S = 2.261(2)). The Cu(II) ion lies at a mean distance of 0.203(1) Å above the equatorial coordination plane (Cl−N2−N1−N2′). Chelation of the bisimpy ligand leads to coplanararity of the imino nitroxyl fragments and the pyridine plane, with a dihedral angle between the two planes of 2.6(2)°. In the noncoordinated dinitronyl and imino nitroxides bridged by phenyl, thiophenyl, and 2,2′-bithienyl groups, the aromatic

(8) (a) Itoh, K. *Chem. Phys. Lett.* **1967**, *1*, 235; b) Sugawara, T.; Bandow, S.; Kimura, K.; Iwamura, H.; Itoh, K. *J. Am. Chem. Soc*. **1986**, *108*, 368. c) Teki, Y.; Takui, T.; Itoh, K.; Iwamura, H.; Kobayashi, K. *J. Am. Chem. Soc*. **1986**, *108*, 2147. d) Fujita, I.; Teki, Y.; Takui, T.; Kinoshita, M.; Itoh K. *J. Am. Chem. Soc*. **1990**, *112*, 4074.

(9) (a) Romero, F. M.; Ziessel, R.; Bonnet, M.; Pontillon, Y.; Ressouche, E.; Schweizer, J.; Delley, B.; Grand, A.; Paulsen, C. *J. Am. Chem. Soc*. **2000**, *122*, 1298. (b) Pontillon, Y.; Caneschi, A.; Gatteschi, D.; Ressouche, E.; Schweizer, J.; Sesssoli, R. *Physica B* **1999**, *267-268*, 51. (c) Ressouche, E.; Boucherle, J.-X.; Gillon, B.; Rey, P.; Schweizer, J. *J. Am. Chem. Soc*. **1993**, *115*, 3610. (d) Zheludev, A.; Barone, V.; Bonnet, M.; Delley, B.; Grand, A.; Ressouche, E.; Rey, P.; Subra, R.; Schweizer, J. *J. Am. Chem. Soc*. **1994**, *116*, 2019. (e) Barone, V.; Bencini, A.; Matteo, A. *J. Am. Chem. Soc*. **1997**, *119*, 10837. (f) Zheludev, A.; Bonnet, M.; Delly, B.; Grand, A.; Luneau, D.; Örström, L.; Ressouche, E.; Rey, P.; Schweizer, J. *J. Magn. Magn. Mater*. **1995**, *145*, 293. (g) Yamaguchi, K.; Fukui, H.; Fueno, T. *Chem. Lett*. **1986**, 625. (h) Yamaguchi, K.; Okumura, M.; Nakano, M. *Chem. Phys. Lett*. **1992**, *191*, 237. (i) Pontillon, Y.; Akita, T.; Grand, A.; Kobayashi, K.; Lelievre-Berna, E.; Pécaut, J.; Ressouche, E.; Schweizer, J. *J. Am. Chem. Soc*. **1999**, *121*, 10126.

(10) Pontillon, Y.; Bencini, A.; Caneschi, A.; Dei, A.; Gatteschi, D.; Gillon, B.; Sangregorio, C.; Stride, J.; Totti, F. *Angew. Chem., Int. Ed*. **2000**, *39*, 1786.

(11) (a) Rancurel, C.; Lezno, D. B.; Sutter, J.-P.; Golhen, S.; Ouahab, L.; Kliava, J.; Kahn, O. *Inorg. Chem*. **1999**, *38*, 4753. (b) Fegy, K.; Sanz, N.; Luneau, D.; Belorizky, E.; Rey, P. *Inorg. Chem*. **1998**, *37*, 4518. (c) de Panthou, F. L.; Luneau, D.; Musin, R.; Öhrström, L.; Grand, A.; Turek, P.; Rey, P. *Inorg. Chem*. **1996**, *35*, 3484.

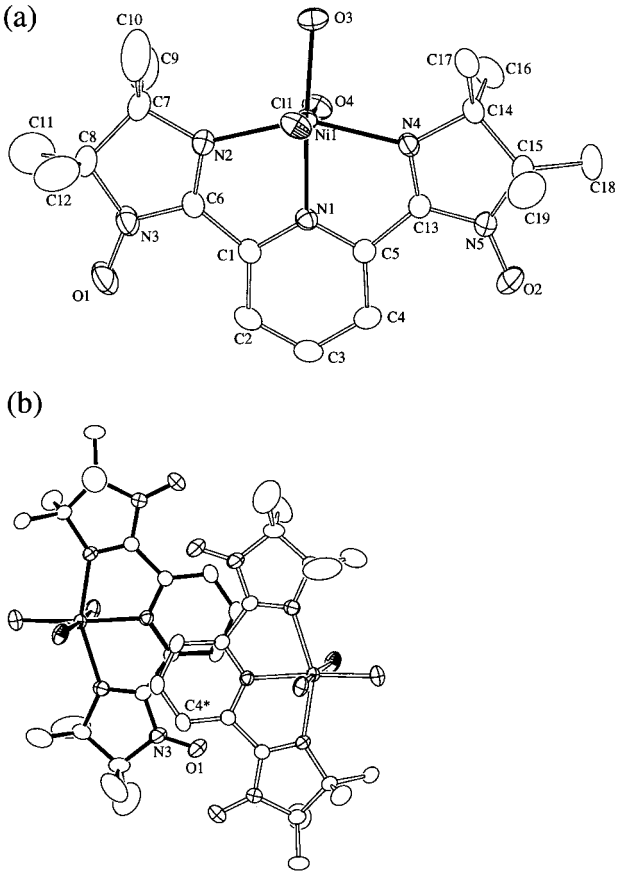

Figure 3. Ortep diagrams (30% probability) of (a) $[NiCl(bisimpy)(H_2O)_2]^+$ (**3**) and (b) the dimeric stack.

Table 1. Selected Bond Lengths [Å] and Angles [deg] for $[CuCl(bisimpy)(MeOH)](PF_6)$ (**1**)[a]

Cu−N(1)	1.979(2)	Cu−N(2)	2.0686(15)
Cu−Cl	2.2226(7)	Cu−O(2S)	2.261(2)
O(1)−N(3)	1.268(2)		
N(1)−Cu−N(2)	78.80(4)	N(2)−Cu−N(2)#1	157.26(8)
N(1)−Cu−Cl	168.89(7)	N(2)−Cu−Cl	100.61(4)
N(1)−Cu−O(2S)	87.65(9)	N(2)−Cu−O(2S)	91.46(4)
Cl−Cu−O(2S)	103.46(6)	C(11S)−O(2S)−Cu	127.5(3)

[a] Symmetry transformations used to generate equivalent atoms: #1 $-x+1, y, z$.

Table 2. Selected Bond Lengths [Å] and Angles [deg] for $[ZnCl_2(bisimpy)]$ (**2**)

Zn(1)−N(1)	2.1551(16)	Zn(1)−Cl(2)	2.2263(6)
Zn(1)−Cl(1)	2.2436(6)	Zn(1)−N(4)	2.2639(16)
Zn(1)−N(2)	2.2881(16)	Zn(2)−N(6)	2.1467(16)
Zn(2)−Cl(4)	2.2250(6)	Zn(2)−Cl(3)	2.2370(6)
Zn(2)−N(9)	2.2770(17)	Zn(2)−N(7)	2.2979(16)
O(1)−N(3)	1.272(2)	O(2)−N(5)	1.267(2)
O(3)−N(8)	1.273(2)	O(4)−N(10)	1.266(2)
O(1)...O(4)	3.760(3)	O(2)...O(3)	3.755(3)
N(1)−Zn(1)−Cl(2)	115.52(5)	N(1)−Zn(1)−Cl(1)	121.67(5)
Cl(2)−Zn(1)−Cl(1)	122.78(2)	N(1)−Zn(1)−N(4)	73.58(6)
Cl(2)−Zn(1)−N(4)	98.99(5)	Cl(1)−Zn(1)−N(4)	94.99(5)
N(1)−Zn(1)−N(2)	73.01(6)	Cl(2)−Zn(1)−N(2)	98.62(5)
Cl(1)−Zn(1)−N(2)	99.19(4)	N(4)−Zn(1)−N(2)	146.37(6)
N(6)−Zn(2)−Cl(4)	118.58(5)	N(6)−Zn(2)−Cl(3)	116.00(5)
Cl(4)−Zn(2)−Cl(3)	125.42(3)	N(6)−Zn(2)−N(9)	73.89(6)
Cl(4)−Zn(2)−N(9)	100.14(5)	Cl(3)−Zn(2)−N(9)	94.23(5)
N(6)−Zn(2)−N(7)	73.18(6)	Cl(4)−Zn(2)−N(7)	97.54(5)
Cl(3)−Zn(2)−N(7)	97.92(5)	N(9)−Zn(2)−N(7)	146.98(6)

rings and imino or nitronyl nitroxyl planes tilt toward each other, with an angle of about 30°.[14]

Complex **2** crystallizes in the monoclinic space group $P2_1/n$.

Table 3. Selected Bond Lengths [Å] and Angles [deg] of $[NiCl(bisimpy)(H_2O)_2]Cl_2 \cdot H_2O$ (**3**)

Ni(1)−O(3)	2.033(2)	Ni(1)−N(1)	2.040(2)
Ni(1)−O(4)	2.106(2)	Ni(1)−N(4)	2.126(2)
Ni(1)−N(2)	2.148(2)	Ni(1)−Cl(1)	2.3870(8)
O(3)−Ni(1)−N(1)	170.95(9)	O(3)−Ni(1)−O(4)	85.33(8)
N(1)−Ni(1)−O(4)	86.14(8)	O(3)−Ni(1)−N(4)	99.65(9)
N(1)−Ni(1)−N(4)	77.20(9)	O(4)−Ni(1)−N(4)	89.19(9)
O(3)−Ni(1)−N(2)	106.43(9)	N(1)−Ni(1)−N(2)	76.60(9)
O(4)−Ni(1)−N(2)	90.23(9)	N(4)−Ni(1)−N(2)	153.78(9)
O(3)−Ni(1)−Cl(1)	90.46(6)	N(1)−Ni(1)−Cl(1)	98.03(7)
O(4)−Ni(1)−Cl(1)	175.74(6)	N(4)−Ni(1)−Cl(1)	90.89(7)
N(2)−Ni(1)−Cl(1)	91.57(6)		

In **2**, there are two crystallographically independent molecules, which stack to form a dimeric unit (Figure 2b).

The coordination geometry about the Zn(II) ions in the two molecules is trigonal bipyramidal, and they also have a similar coordination arrangement about the Zn(II) ion. The equatorial positions are occupied by two chloride ions and a pyridyl nitrogen atom (N1 for Zn1 and N6 for Zn2) from bisimpy. The Zn−Cl and Zn−N(pyridine) bond lengths are 2.2250(6)−2.2436(6) and 2.155(2)−2.147(2) Å, respectively, and the equatorial bond angles about the Zn(II) ions are in the range of 115.52(5)−122.78(2)° for Zn1 and 116.00(5)−125.42(3)° for Zn2. The imino nitrogen atoms of the radicals coordinate to the Zn ions in the apical positions, with bond lengths of 2.264(2)−2.298(2) Å. The imino nitroxyl and pyridyl planes of the bisimpy in **2** are almost coplanar to each other, with a dihedral angle of less than 5.7°.

Complex **3** crystallizes in the triclinic space group of $P\bar{1}$. The Ni(II) ion has a distorted octahedral coordination geometry, of which four coordination sites are coordinated by the bisimpy and chloride ion, and two water molecules occupy the remaining cis positions.

The coordination bond lengths with the iminyl nitrogen atoms (N2 and N4) are 2.126(2) and 2.148(2) Å, and that with the pyridyl nitrogen atom is 2.040(2) Å. The Ni−O4(H_2O) bond trans to the chloride ion shows a slightly longer bond length (2.106(2) Å) than that of the Ni−O3(H_2O) bonds (2.033(2) Å). The Ni−Cl distance is 2.3870(8) Å, which is longer than the other coordination bond lengths (2.033(2)−2.148(2) Å). The radical ligands (bisimpy) in the adjacent molecules have close contacts to form a dimeric unit, of which distances of the N3···C4*, O1···C4*, C1···C2*, and C6···C3* contacts (key to symmetry operation: $1-x, -y, 1-z$) are 3.588(4), 3.527(4), 3.336(3), and 3.449(3) Å, respectively.

Magnetic Properties. Magnetic susceptibility measurements for $[CuCl(bisimpy)(MeOH)](PF_6)$ (**1**), $[ZnCl_2(bisimpy)]$ (**2**), and $[NiCl(bisimpy)(H_2O)_2]Cl \cdot 2H_2O$ (**3**) were performed in the temperature range of 2.0−300 K, and $\chi_m T$ versus T plots are shown in Figures 6, 4, and 7, where χ_m and T represent the molar susceptibility and temperature, respectively.

The $\chi_m T$ value at 300 K for **2** is 0.785 emu mol^{-1} K, which corresponds to the value expected for the uncorrelated two spin system. The $\chi_m T$ values steadily decreased as the temperature was lowered, meaning that there is substantial antiferromagnetic interaction in the high-temperature region.

(12) (a) Belorizky, E.; Rey, P.; Luneau, D. *Mol. Phys.* **1998**, *94*, 643. (b) Luneau, D.; Laugier, J.; Rey, P.; Lrich, G.; Ziessel, R.; Legoll, P.; Drillon, M. *J. Chem. Soc., Chem. Commun.* **1994**, 741. (c) Oshio, H.; Yaginuma, T.; Ito, T. *Inorg. Chem.* **1999**, *38*, 2750. (d) Oshio, H.; Yamamoto, M.; Ito, T. *J. Chem. Soc., Dalton Trans.* **1999**, 2641.
(13) (a) Inoue, K.; Iwamura, H. *J. Am. Chem. Soc.* **1994**, 116, 3173.
(14) (a) Mitsumori, T.; Inoue, K.; Koga, N.; Iwamura, H. *J. Am. Chem. Soc.* **1995**, *117*, 2467. (b) Oshio, H.; Umeno, M.; Fukushi, T.; Ito, T. *Chem. Lett.* **1997**, 1065.

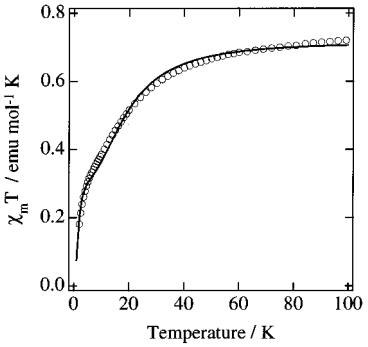

Figure 4. $\chi_m T$ versus T plot of [$ZnCl_2$(bisimpy)] (**2**). The solid line corresponds to the theoretical curves, of which parameters are given in the text.

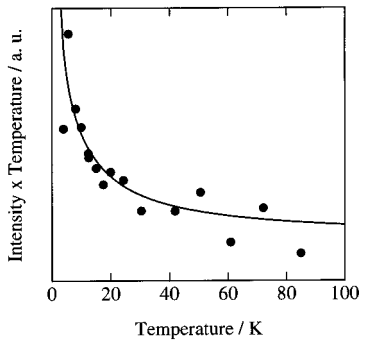

Figure 5. Temperature dependence of EPR signal intensity of the $\Delta m_s = 2$ transition for [ZnCl2(bisimpy)] (**2**). The solid line was obtained using a modified Bleaney−Bowers equation.

In organic multiradical compounds, a spin polarization mechanism is useful in predicting the sign of the magnetic interaction between radical centers. Because bisimpy has two imino nitroxyl groups linked at the meta position of the pyridine group, the condition necessary for the intraligand ferromagnetic interaction is met. Since the antiferromagnetic interaction was observed for **2**, there must be an anitferromagnetic pathway which overcomes the intraligand ferromagnetic interaction. In **2**, the two independent molecules stack to form a dimeric structure with a parallel arrangements, in which dihedral angles of the stacked imino nitroxyl groups are 2.6(2) and 10.8(2)°, and the interradical (O1···O4, O1···N10, O3···O2, and O3···N5) distances are 3.535(3)−3.760(3) Å. This arrangement of SOMO−SOMO overlaps (SOMO = singly occupied molecular orbital) favors an antiferromagnetic intradimer interaction. The X-band EPR spectrum of a frozen ethanol solution of **2** was measured in order to exclude any intermolecular magnetic interactions. The EPR spectrum shows typical triplet signals with axial symmetry having intense signals at 0.33−0.35 T and a well resolved half-field signal at 0.16 T. The zero-field splitting parameter $|D|$ was calculated to be 0.0067 cm^{-1}.[15] The temperature dependence of the signal intensity for the $\Delta m_s = 2$ transition was measured in the temperature range of 6−85 K, and the result is shown in Figure 5.

Because the value of the intensity times temperature increased as the temperature was lowered, the intramolecular magnetic interaction was determined to be ferromagnetic. The temperature variations of the EPR intensity data were used to estimate the intramolecular ferromagnetic interaction using a modified Bleaney−Bowers equation ($H = -2JS_1S_2$),[16] and a J value of +6.5(9) cm^{-1} was obtained. In the dimeric unit of **2**, there are four imino nitroxyl groups with intramolecular ferromagnetic and intermolecular antiferromagnetic interactions. Magnetic data of **2** was analyzed by a four spin model, of which the theoretical expression was derived by Hatfield.[17] The exchange coupling constants J_1 and J_2, representing intra- and interligand magnetic interactions, respectively, were used in the calculation. The least squares calculation with the fixed g value of 2.0 yielded the best fit J_1 and J_2 values of +8.4(1) and −15.7(4) cm^{-1}, respectively.

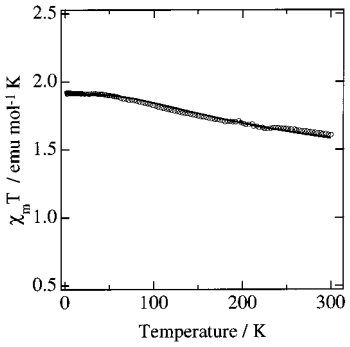

Figure 6. $\chi_m T$ versus T plot of [CuCl(bisimpy)(MeOH)](PF_6) (**1**). The solid line corresponds to the theoretical curves, of which parameters are given in the text.

Scheme 1

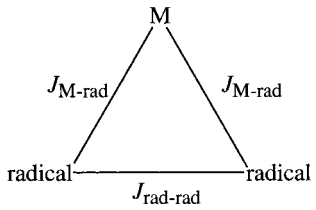

M = Cu or Ni

The temperature dependence of the $\chi_m T$ values for **1** showed quite different behavior from that of **2** (Figure 6). The Cu(II) ion has an unpaired electron in a $d_{x^2-y^2}$ orbital, and the bisimpy ligand has two radical moieties. The value of $\chi_m T$ at 300 K was 1.60 emu mol^{-1} K, which is higher than the value (1.125 emu mol^{-1} K) expected for an uncorrelated three spin system.

The values of $\chi_m T$ increased as the temperature was lowered and reached a plateau value of 1.89 emu mol^{-1} K at 40 K. Since the Curie constant for the $S = 3/2$ state is 1.876 emu K mol^{-1}, with $g = 2.0$, it was concluded that the three-half spins in **1** have a parallel alignment below 40 K. The ferromagnetic interaction between the Cu(II) ion and radical moieties is due to the orthogonality of the $d_{x^2-y^2}$ and pp orbitals, and the intraligand ferromagnetic interaction is also predicted by the spin-polarization mechanism. The two exchange parameters J_{Cu-rad} and $J_{rad-rad}$ for the Cu(II)−radical and intraligand magnetic interactions were introduced for the analysis of the magnetic data (Scheme 1).

Using the spin Hamiltonian $H = -2J_{Cu-rad}(2S_{Cu}S_{radical}) - 2J_{rad-rad}S_{radical}S_{radical}$, the molar susceptibility was calculated using the following

(15) (a) Kottis, P.; Lefebvre, R. *J. Chem. Phys*. **1963**, *39*, 393. (b) Kottis, P.; Lefebvre, R. *J. Chem. Phys*. **1964**, *41*, 379.

(16) Bleaney, B.; Bowers, K. D. *Proc. R. Soc. London, Ser. A* **1952**, *214*, 451.

(17) Hall, J. W.; Estes, W. E.; Estes, E. D.; Scaringe, R. P.; Hatfield, W. E. *Inorg. Chem.* **1977**, *16*, 1572.

$$\chi_m = \frac{N\beta^2}{4kT} \times \frac{10{g_1}^2 \exp(J_{\mathrm{Cu-rad}}/kT) + {g_2}^2 \exp(-2J_{\mathrm{Cu-rad}}/kT) + {g_3}^2 \exp(-2J_{\mathrm{rad-rad}}/kT)}{2\exp(J_{\mathrm{Cu-rad}}/kT) + \exp(-2J_{\mathrm{Cu-rad}}/kT) + \exp(-2J_{\mathrm{rad-rad}}/kT)}$$

$$g_1 = \frac{1}{3}(g_{\mathrm{Cu}} + 2g_{\mathrm{rad}})$$

$$g_2 = \frac{1}{3}(-g_{\mathrm{Cu}} + 4g_{\mathrm{rad}})$$

$$g_3 = g_{\mathrm{Cu}}$$

It is difficult to determine the amplitude of the coupling constants for a triangularly aligned three spin system. Assuming fairly strong intraligand ferromagnetic interactions, i.e., when $J_{\mathrm{rad-rad}}$ is larger than 300 cm^{-1} and bisimpy acts as a triplet radical, $J_{\mathrm{Cu-rad}}$ becomes $+52$ cm^{-1}. This might be consistent with the fact that the $\chi_m T$ value (1.60 emu mol^{-1} K) at 300 K is higher than the value expected (1.375 emu mol^{-1} K) for a magnetically separated Cu(II) doublet and triplet diradical. On the other hand, when the two imino nitroxides in bisimpy are weakly coupled as in **2**, the exchange coupling constant $J_{\mathrm{Cu-rad}}$ between the Cu(II) ion and radical was estimated to be $+165$-(1) cm^{-1} with a g_{Cu} value of 2.017(1), where the $J_{\mathrm{rad-rad}}$ and g_{radical} values were fixed at $+6.5$ cm^{-1} and 2.0, respectively. It is impossible to determine which description is appropriate from only the magnetic data. Using DFT molecular orbital calculation, the intraligand ferromagnetic interaction was determined to be weak, and the values of $J_{\mathrm{Cu-rad}}$ and $J_{\mathrm{rad-rad}}$ were concluded to be 165(1) and 6.5 cm^{-1}, respectively. Details are discussed in the following section.

The temperature variation of $\chi_{\mathrm{m}}T$ values for **3** is depicted in Figure 7. The $\chi_{\mathrm{m}}T$ value at 300 K is 2.93 emu mol K^{-1}, which is slightly higher than the value expected for isolated Ni(II) ($S = 1$) and two radical ($S = 1/2$) spins. The $\chi_{\mathrm{m}}T$ values showed a gradual increase as the temperature was lowered and reached the plateau value (3.34 emu mol K^{-1}) at 55 K, which is followed by sudden increase at 15 K.

The temperature dependence of the χ_{m}T values above 55 K is indicative of the intramolecular ferromagnetic interactions being operative, and the complex molecule **3** has the $S = 2$ spin ground state. The occurrence of the ferromagnetic interaction was understood by the fact that the magnetic orbitals of the Ni(II) ion are orthogonal to those of the coordinated imino nitroxide. As the temperature was lowered below 15 K, the $\chi_{\mathrm{m}}T$ values suddenly increased, which implies the intermolecular magnetic interactions are ferromagnetic. In bisimpy, the positive spins mainly populate the nitroxyl groups and iminyl nitrogen atoms, and negative and positive spins are alternatly aligned in the pyridyl group (see the DFT result on bisimpy). The X-ray structural analysis for **3** showed a two complex molecule form dimeric structure with close contacts of nitroxyl group (O1 and N3) and pyridyl carbon atom (C4*) in the next molecule (Figure 3b), and these carry positive and negative spins, respectively. This dimeric stacking mode matches McConnell's criteria,[18] which leads to the intermolecular ferromagnetic interaction. The magnetic susceptibility data was analyzed by the triangular model (Scheme 1), of which exchange parameters $J_{\mathrm{Ni-rad}}$ and $J_{\mathrm{rad-rad}}$ correspond to the Ni(II)−radical and intraligand magnetic interactions. The formula used in the calculation was derived by the Kambe's vector model,[19] and it includes intradimer magnetic interaction as θ.

(18) McConnel, H. M. *J. Chem. Phys.* **1963**, *39*, 1910.
(19) Kambe, K. *J. Phys. Soc. Jpn*. **1950**, *5*, 48.

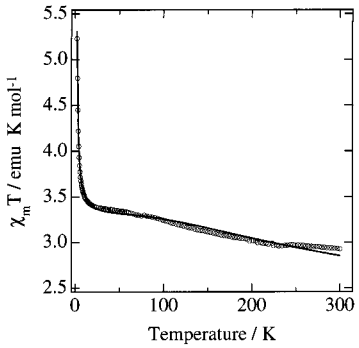

Figure 7. $\chi_{\mathrm{m}}T$ versus T plot of $[NiCl(bisimpy)(H_2O)_2]Cl{\cdot}2H_2O$ (**3**). The solid line corresponds to the theoretical curves, of which parameters are given in the text.

$$\chi_m = \frac{N\beta^2}{k(T-\theta)} \times \frac{10{g_1}^2 + 2{g_1}^2 \exp[-4J_{\mathrm{Ni-rad}}/kT] + 2{g_2}^2 \exp[(-2J_{\mathrm{Ni-rad}} - 2J_{\mathrm{rad-rad}})/kT]}{5 + 3\exp[-4J_{\mathrm{Ni-rad}}/kT] + 3\exp[(-2J_{\mathrm{Ni-rad}} - 2J_{\mathrm{rad-rad}})/kT] + \exp[-6J_{\mathrm{Ni-rad}}/kT]}$$

$$g_1 = (g_{\mathrm{Ni}} + g_{\mathrm{rad}})/2$$

$$g_2 = g_{\mathrm{Ni}}$$

The least squares calculation yielded the best fit parameters of the $J_{\mathrm{Ni-rad}}$, g_{Ni}, and θ values as 109(2) cm^{-1}, 2.166(3), and 0.8-(1) K, respectively. In this calculation, the $J_{\mathrm{rad-rad}}$ and g_{rad} values were fixed to 6.5 cm^{-1} and 2.0, respectively. Recently, the Ni-(II) complexes with diradicals of nitronyl nitroxides were prepared. Magnetic interactions between the Ni(II) ions and the coordinated nitronyl nitroxides varied from antiferromagnetic[25a] (-240 cm^{-1}) to ferromagnetic[3c] (6.9−39.6 cm^{-1}) interactions, and it is concluded that the different coordination bond angles of Ni(II)−O−N(nitroxides) are responsible for the magnetic interactions.

DFT Calculations. We performed DFT calculations for the free ligand bisimpy (**L**), $[CuCl(bisimpy)(MeOH)](PF_6)$ (**1**), and $[ZnCl_2(bisimpy)]$ (**2**), to obtain the J values shown in Table 6. Mulliken spin populations and charge densities for **L**, **1**, and **2**, together with a numbering scheme, are summarized in Tables 4 and 5, and their spin population maps are shown in Figure 8. Natural population analysis also yielded similar results. The detailed computational methods are given in the Experimental Section.

Intraligand Ferromagnetic Interaction. The spin density of radical ligands **L**, **1**, and **2** is localized mainly on the imino

(20) (a) Cogne, A.; Grand, A.; Rey, P.; Subra, R. *J. Am. Chem. Soc*. **1989**, *111*, 3230. (b) Adam, D. M.; Rheingold, A. L.; Dei, A.; Hendrickson, D. N. *Angew. Chem., Int. Ed. Engl*. **1993**, *32*, 391. (c) Caneschi, A.; Dei, A.; Gatteschi, D. *J. Chem. Soc., Chem. Commun*. **1992**, 630. (d) Bruni, S.; Caneschi, A.; Cariati, F.; Delfs. C.; Dei, A.; Gatteschi, D. *J. Am. Chem. Soc*. **1994**, *116*, 1388.
(21) (a) Fox, G. A.; Pierpont, C. G. *Inorg. Chem*. **1992**, *31*, 3718. b) Abakumov, G. A.; Cherkasov, V. K.; Bubnov, M. P.; Ellert, O. G.; Rakitin, U. V.; Zakharov, L. N.; Struchkov, Y. T.; Saf'yanov, U. N. *Isv. Akad. Nauk SSSR* **1992**, 2315. c) Oshio, H.; Ohto, A.; Ito, T. *Chem. Commun*. **1996**, 1541.
(22) (a) Francese, C.; Romero, F. M.; Neels, A.; Stoeckli-Evans, H.; Decurtins, S. *Inorg. Chem*. **2000**, *39*, 2095. (b) Oshio, H.; Watanabe, T.; Ohto, A.; Ito, T.; Ikoma, T.; Tero-Kubota, S. *Inorg. Chem*. **1997**, *36*, 3014. (c) Lange, C. W.; Conklin, B. J.; Pierpont, C. G. *Inorg. Chem*. **1994**, *33*, 1276.
(23) (a) Musin, R. N.; Ovcharenko, I. V.; Öhrström. L.; Rey, P. *J. Struct. Chem*. **1997**, *38*, 703. b) Musin, R. N.; Ovcharenko, I. V.; Öhrström. L.; Rey, P. *J. Struct. Chem*. **1997**, *38*, 712.
(24) Ulrich, G.; Ziessel, R. *Tetrahedron Lett*. **1994**, *35*, 1215.
(25) Hatfield, W. E. *Theory and Application of Molecular Paramagnetism*; Boudreaux, E. A., Mulay, L. N. Eds.; Wiley and Sons: New York, 1976; pp 491−495.

Table 4. Atomic Spin Population (Charge Distribution in Parentheses) Obtained by DFT Calculations[a,b]

	bisimpy	$[ZnCl_2(bisimpy)]$	$[CuCl(bisimpy)]^+$
Cu			+0.558
			(+0.552)
Zn		−0.009	
		(+0.752)	
O	+0.495	+0.507	+0.531
	(−0.418)	(−0.386)	(−0.343)
N1	+0.325	+0.292	+0.238
	(−0.116)	(−0.081)	(−0.078)
N2	+0.340	+0.330	+0.408
	(−0.434)	(−0.486)	(−0.503)
N3	−0.041	−0.035	+0.046
	(−0.505)	(−0.600)	(−0.613)
C1	−0.147	−0.125	−0.095
	(+0.498)	(+0.512)	(+0.530)
C2	+0.039	+0.033	+0.026
	(+0.262)	(+0.308)	(+0.301)
C3	−0.047	−0.041	−0.035
	(−0.110)	(−0.101)	(−0.077)
C4	+0.026	+0.022	+0.016
	(−0.072)	(−0.059)	(−0.063)
C5	−0.015	−0.015	−0.014
	(−0.172)	(−0.166)	(−0.175)
C6	−0.022	−0.019	−0.012
	(−0.152)	(−0.158)	(−0.161)
Cl1		+0.010	+0.201
		(−0.536)	(−0.373)
Cl2		+0.012	
		(−0.525)	

[a] Listed spin populations are calculated values for the triplet states of bisimpy and $[ZnCl_2(bisimpy)]$, and for the quartet state of $[CuCl(bisimpy)]^+$. [b] Atomic numbering scheme for this table:

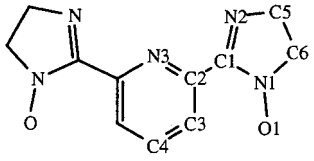

Table 5. Spin Populations in σ and π Orbitals at the Selected Atoms;[a] the Numbers in Parentheses for the Complex are the Differences from Bisimpy

	bisimpy		$[CuCl(bisimpy)]^+$	
	σ	π	σ	π
Cu			+0.524	+0.034
O	+0.027	+0.467	+0.020	+0.511
			(−0.007)	(+0.044)
N1	+0.034	+0.290	+0.014	+0.224
			(−0.020)	(−0.066)
N2	+0.033	+0.307	+0.117	+0.291
			(+0.084)	(−0.016)
N3	−0.006	−0.035	+0.059	−0.013
			(+0.065)	(+0.022)
Cl			+0.170	+0.032

[a] For atomic numbering scheme used for this table see Table 4.

nitroxyl groups (O−N1−C1−N2). Strong positive spin populations are found on the iminyl nitrogen (N2) and nitroxide group (O−N1), and negative spin populations are observed on the bridging sp^2 carbon atom (C1). Intramolecular magnetic interactions between the coordinated imino nitroxides are mediated by the metal ion and the pyridine group. Recently, moderate ferro-[20] and antiferromagnetic[21] interactions of organic radicals bound to diamagnetic metal ions were reported. For example, a titanium(IV) complex TiL_2 (L = tridentate dianion of semiquinone ligand) showed a ferromagnetic interaction (J = +56 cm^{-1}) between the coordinated semiquinones through the diamagnetic Ti^{4+} ion.[10] Polarized neutron diffraction (PND) and

Table 6. Exchange Parameters [J, cm^{-1}] by Magnetic Measurements and DFT Calculations[a]

	J[b] exptl. (DFT calcd.)	J_1[b] exptl. (DFT calcd.)	J_2[b] exptl. (DFT calcd.)
bisimpy			
	(+21.6)		
$[ZnCl_2(bisimpy)]$ (**2**)	6.5		
	(16.3)		
$[CuCl(bisimpy)(MeOH)](PF_6)$ (**1**)		165(1)	6.5[c]
		(216.2)	(48.8)

[a] In the DFT calculations, the methyl groups of bisimpy were replaced by hydrogen atoms. [b] The exchange coupling constant, J, represents the intraligand coupling constant in bisimpy and 2, while the J_1 and J_2 correspond to the exchange coupling constants for the Cu^{2+} radical and inter-radical interactions, respectively, in **1**. [c] Assumed to be the same for the J value of **2**.

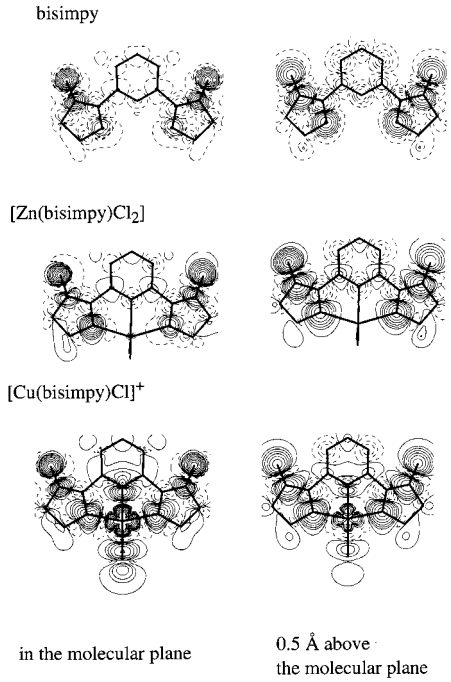

Figure 8. Spin density maps projected onto the molecular plane (left-hand side) and 0.5 Å above the molecular plane (right-hand side) for free ligand **L**, **1**, and **2**: positive contours (−) and negative contours (- - --). In the DFT calculations, methyl groups in the imino nitroxides were replaced by hydrogen atoms.

DFT studies on TiL_2 revealed a substantial positive spin population localized on the Ti^{4+} ion, which acts as a mediator for the ferromagnetic interaction. It was shown that a charge transfer interaction partially transfers the radical spin to the diamagnetic metal ion, and this plays an important role in the propagation of the magnetic interactions.[22,23] In **2** and $[Zn(2,6\text{-}NITpy)_2](ClO_4)$ (2,6-NITpy = diradical of nitronyl nitroxide),[23a] inter-radical magnetic interactions are very weak, and the DFT results for **2** showed negligibly small spin delocalization on the Zn^{2+}. In **2**, the magnetic interaction through the Zn(II) ion is extremely small, and this is due to a very high-energy charge transfer state between the Zn(II) ion and an imino nitroxyl group. On the other hand, the spin populations on the pyridyl groups in **L**, **1**, and **2** were not substantial either, although positive and negative spins are alternately aligned in the pyridine groups. The spin polarization mechanism is not an effective description for the diradical ligand studied, which is understandable due to the relatively small negative spin density on the bridging carbon atom (C1).

Ferromagnetic Interaction between the Copper(II) Ion and Radical. The ferromagnetically coupled **1** has substantial spin populations on the Cu^{2+} and Cl^- ions and imino nitroxyl groups (O−N1−C1−N2, see numbering in Table 4; Figure 8, Tables 4 and 5), and the total spin population on imino nitroxyl groups in **1** (+1.082) is larger than those in **L** and **2** (+0.977 and +1.004, respectively). On the other hand, the total charge on the imino nitroxyl groups in **1** (−0.394) is less negative compared with those in **L** and **2**, −0.470 and −0.441, respectively, and the positive charge of +0.552 on the Cu(II) ion is smaller than that of +0.752 on the Zn(II) ion. These results suggest that in **1**, electron transfer takes place from imino nitroxide to the Cu(II) ion, increasing the spin on the imino nitroxyl group. Table 5 shows in more detail what happens upon coordination of **L** to the Cu(II) ion. The spin populations in the σ orbitals of N2 and N3 which coordinate to the Cu(II) ion increase. This result and the spin density in Figure 8 show β electron transfers from the pσ orbitals of these nitrogen atoms to the $d_{x^2-y^2}$ orbital of the Cu(II) ion. This electron transfer induces larger spin polarization in the nitroxy group in which the positive spin density in the pπ orbital on the O atom increases and that on the N1 atom decreases.

As just discussed, a LMCT (from a pσ to a $d_{x^2-y^2}$ orbital) interaction induces a spin in the ligand pσ orbitals, which are orthogonal to the SOMO (pπ orbital) of the imino nitroxide itself. Recently, ab initio analyses of the spin population were reported for a ferromagnetically coupled Cu(II)−radical complex, Cu(II)L_2 (L = enaminoketone 3-imidazoline nitroxides), which showed a ferromagnetic interaction of $J = +18$ cm^{-1} ($H = -2JS_iS_j$) between the Cu(II) ion and the nitroxides.[23] The principle mechanism of exchange interactions in CuL_2 system was suggested to be delocalization mediated by a minor transfer of spin density from the dσ orbital of Cu(II) ion (such as $d_{x^2-y^2}$ in **1**) to the pσ orbital of the nitroxide groups, and this is in accord with our conclusion.

Estimation of the Exchange Coupling Constants. The interradical coupling constant J for **L** and **2** were calculated to be 21.6 and 16.3 cm^{-1}, respectively (Table 6). These small positive values qualitatively accord with the experimental J value (6.5 cm^{-1}) for **2**, though they are about three times larger. In **1**, on the other hand, three-half spins from the Cu(II) ion and two imino nitroxides are ferromagnetically coupled, leading to a quartet ground state. There are two doublet states above the quartet state, and energy levels from the ground quartet state are, respectively, $J_1 + 2J_2$ and $3J_1$, where J_1 and J_2 correspond to the coupling constants for the Cu(II)−radical and radical−radical interactions. The energy levels of the two doublet states depend on amplitudes of the J_1 and J_2 values, and the analysis of the experimental magnetic data for **1** is not straightforward.

The DFT calculation for **L**, **1**, and **2** showed a small spin population on the pyridyl groups. It is reasonable to suppose that the intraligand ferromagnetic interactions in **L**, **1**, and **2** are similarly weak. In the analysis of the experimental magnetic data of **1**, the intraligand magnetic interaction ($J_{rad-rad}$) was, therefore, fixed to +6.5 cm^{-1}, and a J_{Cu-rad} value of 165(1) cm^{-1} was obtained. It should be noted that DFT calculations for **1** gave J_{Cu-rad} and $J_{rad-rad}$ values of 216.2 and 48.8 cm^{-1}, respectively. While the theoretical values are in qualitative agreement with the experimental values, understanding of the discrepancy of the experimental and DFT calculated J_{Cu-rad} and $J_{rad-rad}$ values requires further theoretical investigation.

In conclusion, the Cu(II) and Ni(II) complexes with the diradical ligands have the spin quartet and quintet ground states, respectively, and the fairly strong ferromagnetic interactions are operative due to the orthogonality of the Cu(II) and Ni(II) dσ orbitals with imino nitroxide pπ orbitals. It should be noted that the spin population of the diradical ligand in this system changed by only a small amount upon coordination to the metal ions.

Table 7. Crystal data for [CuCl(bisimpy)(MeOH)](PF_6) (**1**), [$ZnCl_2$(bisimpy)] (**2**), and [NiCl(bisimpy)(H_2O)$_2$]Cl·2H_2O (**3**)

	1	2	3
chemical formula	$C_{20}H_{31}ClCuF_6N_5O_3P$	$C_{19}H_{27}Cl_2N_5O_2Zn_1$	$C_{19}H_{35}Cl_2N_5Ni_1O_6$
formula weight	633.46	493.73	559.13
space group	*Cmc*2$_1$ (No. 36)	*P*2$_1$/*n* (No. 14)	$P\bar{1}$ (No. 2)
a [Å]	15.8165(9)	15.097(3)	6.5936(2)
b [Å]	13.1367(7)	12.349(3)	13.2244(4)
c [Å]	12.9107(7)	24.260(5)	16.2682(5)
α [°]			108.1630(10)
β [°]		98.14(3)	100.6760(10)
γ [°]			92.6140(10)
vol [Å^3]	2682.5(3)	4477.3(16)	1316.38(7)
Z	4	8	2
ρ [Mg/m^3]	1.568	1.659	1.411
temp [°C]	−70	−70	−70
μ [mm^{-1}]	1.047	1.361	1.084
trans coeff	0.899−1.000	0.898−1.000	0.767−1.000
final *R* indices[a]	R1 = 0.0242	R1 = 0.0328	R1 = 0.0431
[$I > 2\sigma(I)$][b]	wR2 = 0.0649	wR2 = 0.0912	wR2 = 0.1085

[a] $R1 = \sum||F_o| - |F_c||/\sum|F_o|$. [b] $wR2 = [\sum[w(F_o^2 - F_c^2)^2]/\sum[w(F_o^2)^2]]^{0.5}$, calcd. $w = 1/[\sigma^2(F_o^2) + (0.0466P)^2 + 0.3451P]$, $w = 1/[\sigma^2(F_o^2) + (0.0523P)^2 + 1.4891P]$, and $w = 1/[\sigma^2(F_o^2) + (0.0569P)^2 + 1.3938P]$ for **1**, **2**, and **3**, respectively, where $P = (F_o^2 + 2F_c^2)/3$.

Experimental Section

Preparation of Complexes. Chemicals were obtained from standard sources and were used as received.

Bisimpy. 2,6-bis(1′-oxyl-4′,4′,5′,5′-tetramethyl-4′,5′-dihydro-1′*H*-imidazol-2′-yl)pyridine was prepared by the reported method.[24]

[CuCl(bisimpy)(MeOH)](PF_6) (1). Bisimpy (181 mg, 0.5 mmol) was added to a methanol solution (5 mL) of $CuCl_2$·2H_2O (85 mg, 0.5 mmol). Addition of NH_4PF_6 (82 mg) gave dark red needles, one of which was subjected to the X-ray structural analysis. (Found: C, 37.82; H, 4.91; N, 10.96%. $C_{20}H_{31}ClCuF_6N_5O_3P$ requires C, 37.92; H, 4.93; N, 11.06%).

[$ZnCl_2$(bisimpy)] (2). The reaction of bisimpy (181 mg, 0.5 mmol) with $ZnCl_2$ (68 mg, 0.5 mmol) in ethanol gave a red powder. Recrystallization in methanol gave dark red plates, one of which was subjected to the X-ray structural analysis. (Found: C, 46.29; H, 5.39; N, 14.00%. $C_{19}H_{27}Cl_2N_5O_2Zn$ requires C, 46.20 H, 5.51; N, 14.18%)

[NiCl(bisimpy)(H_2O)$_2$]Cl·2H_2O (3). Bisimpy (181 mg, 0.5 mmol) in nitromethane (5 mL) was added to a solution (5 mL) of [$(C_2H_5)_4N]_2$-[$NiCl_4$] (230 mg, 0.5 mmol). After storage in a refrigerator for one night, the red microcrystalline sample was collected by suction. Recrystallization from hot nitromethane yielded dark red tablets, one of which was subjected to the X-ray structural analysis. (Found: C, 40.80; H, 6.25; N, 12.55%. $C_{19}H_{35}Cl_2N_5NiO_6$ requires C, 40.81; H, 6.31; N, 12.53%).

Magnetic Measurements. Magnetic susceptibility data were collected in the temperature range of 2.0−300 K, in an applied field of 5 kG on a Quantum Design model MPMS SQUID magnetometer. Pascal's constants were used to determine the diamagnetic corrections.[25] The X-band EPR spectra of frozen ethanol solutions were recorded at various temperatures between 5.0 and 80 K with a Bruker spectrometer (ESP-300E), which equipped with a helium continuous-flow cryostat, a Hall probe, and a frequency meter.

X-ray Structure Analyses. A dark red needle (0.2 × 0.2 × 0.3 mm^3) of **1**, a dark red plate (0.1 × 0.1 × 0.3 mm^3) of **2**, and a dark red plate (0.2 × 0.2 × 0.3 mm^3) of **3** were mounted with epoxy resin on the tip of a glass fiber (Table 7). Diffraction data were collected at −70 °C on a Bruker SMART 1000 diffractometer fitted with a CCD-

type area detector, and a full sphere of data were collected using graphite-monochromated Mo Kα radiation ($\lambda = 0.71073$ Å). At the end of data collection, the first 50 frames of data were recollected to establish that the crystal had not deteriorated during the data collection. The data frames were integrated using SAINT and were merged to give a unique data set for structure determination. Total reflections collected were 8442, 30404, and 9944 for **1**, **2**, and **3**, respectively, of which independent reflections were 3140 ($R_{int} = 0.0188$), 9983 ($R_{int} = 0.0226$), and 5152 ($R_{int} = 0.0254$). Empirical absorption corrections by SADABS (G. M. Sheldrick, 1994) were carried out ($T_{min}-T_{max}$ values for **1**, **2**, and **3** are 0.899−1.000, 0.898−1.000, and 0.767−1.000, respectively). Crystallographic data are listed in Table 7. The structures were solved by direct methods and refined by the full-matrix least-squares method on all F^2 data using the SHELXTL 5.1 package (Bruker Analytical X-ray Systems). Non-hydrogen atoms were refined with anisotropic thermal parameters. Hydrogen atoms were included in calculated positions and refined with isotropic thermal parameters riding on those of the parent atoms.

DFT Calculations. DFT calculations for the free ligand bisimpy (**L**), [CuCl(bisimpy)(MeOH)](PF_6) (**1**), and [$ZnCl_2$(bisimpy)] (**2**) were performed using GAUSSIAN 98.[26] The Becke3LYP hybrid functional was used throughout this work. The LANL2DZ basis functions and effective core potentials for Cu and Zn, developed by Hay and Wadt,[27] and 6-31G* basis functions for C, H, N, and O atoms were used in every calculation.[28] Geometry of the compounds was taken from the X-ray analyses, geometry optimizations were not performed, and the methyl groups in the imino nitroxides were replaced with hydrogen atoms.

In calculating the J values we adopted the scheme developed by Yamaguchi and co-workers,[29] which was derived using the approximate spin-projection procedure by combination of the molecular orbital or DFT methods with the Heisenberg model. In this scheme, the J values are calculated by dividing the difference in energy between the high and low spin states by the difference in the expectation value of total spin angular momentum, $\langle s^2 \rangle$:

$$\frac{E^{LS} - E^{HS}}{\langle s^2 \rangle^{HS} - \langle s^2 \rangle^{LS}}$$

Since the spin contamination is especially large in the determinants for low-spin states, it is necessary to perform the spin-projection. The expectation values of total spin angular momentum were, in fact, calculated to be 1.043, 1.042, 1.788 for singlet **2**, **L**, and doublet **1**, respectively, whereas those for the high spin states are close to 2.0 or 3.75, a value for a pure spin state. The J value for **L** and **2**, with the spins at the two separated sites, can be obtained with this equation. On the other hand, for **1** there are two states with the different spin distributions radical(↑)−Cu(↓)−radical(↑) and radical(↑)−Cu(↑)−radical-(↓). The former and the latter correspond to the upper and lower doublet states, respectively, shown in Scheme 2. Using the energy and $\langle s^2 \rangle$ for the former doublet state and the quartet state in the above equation, the J_1 value in Scheme 2 is obtained, whereas with those for the latter doublet state, the above equation gives $(J_1 + 2J_2)/3$. Thus, we can know the J_1 and J_2 values by referring the energy and $\langle s^2 \rangle$ values for these two doublet states and the quartet state.

Scheme 2

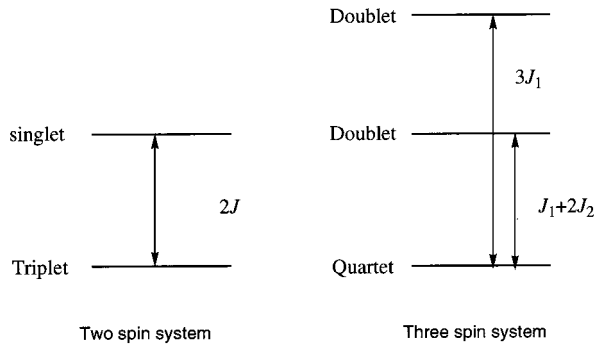

Acknowledgment. This work was in part supported by a Grant in aid for Scientific Research from the Ministry of Education, Science, and Culture, Japan.

Supporting Information Available: X-ray crystallographic files in CIF format for the structure determination of compounds **1**, **2**, and **3**. This material is available free of charge via the Internet at http://pubs.acs.org.

IC0102384

(26) Frisch, M. J.; Trucks, G. W.; Schlegel, H. B.; Scuseria, G. E.; Robb, M. A.; Cheeseman, J. R.; Zakrzewski, V. G.; Montgomery, J. A., Jr.; Stratmann, R. E.; Burant, J. C.; Dapprich, S.; Millam, J. M.; Daniels, A. D.; Kudin, K. N.; Strain, M. C.; Farkas, O.; Tomasi, J.; Barone, V.; Cossi, M.; Cammi, R.; Mennucci, B.; Pomelli, C.; Adamo, C.; Clifford, S.; Ochterski, J.; Petersson, G. A.; Ayala, P. Y.; Cui, Q.; Morokuma, K.; Malick, D. K.; Rabuck, A. D.; Raghavachari, K.; Foresman, J. B.; Cioslowski, J.; Ortiz, J. V.; Stefanov, B. B.; Liu, G.; Liashenko, A.; Piskorz, P.; Komaromi, I.; Gomperts, R.; Martin, R. L.; Fox, D. J.; Keith, T.; Al-Laham, M. A.; Peng, C. Y.; Nanayakkara, A.; Gonzalez, C.; Challacombe, M.; Gill, P. M. W.; Johnson, B. G.; Chen, W.; Wong, M. W.; Andres, J. L.; Head-Gordon, M.; Replogle, E. S.; Pople, J. A. *Gaussian 98*, revision A.6; Gaussian, Inc.: Pittsburgh, PA, 1998.

(27) (a) Hay, J. P.; Wadt, W. R. *J. Chem Phys*. **1985**, *82*, 270. (b) Hay, J. P.; Wadt, W. R. *J. Chem. Phys*. **1985**, *82*, 299.

(28) Hehre, W. J.; Radom, L.; Schleyer, P. V. R.; Pople, J. A. *Ab Initio Molecular Orbital Theory*; Wiley: New York, 1986.

(29) (a) Yamaguchi, K.; Jensen, F.; Dorigo, A.; Houk, K. N. *Chem. Phys. Lett*. **1988**, *149*, 537. (b) Yamaguchi, K.; Fukui, H.; Fueno, T. *Chem. Lett*. **1986**, 625. (c) Mitani, M.; Mori, H.; Takano, Y.; Yamaki, D.; Yoshioka, Y.; Yamaguchi, K. *J. Chem. Phys.* **2000**, 113, 4035. (d) Takano, Y.; Soda, T.; Kitagawa, Y.; Yoshioka, Y.; Yamaguchi, K. *Chem. Phys. Lett.* **1999**, *301*, 309. (e) Yamaguchi, K.; Tsunekawa, T.; Toyoda, Y.; Fueno, T. *Chem. Phys. Lett.* **1988**, *143*, 371. (f) Yamanaka, S.; Kawakami, T.; Nagao, H.; Yamaguchi, K. *Chem. Phys. Lett.* **1994**, *231*, 25.